

# *High Reliability Lead-free Alloys for Performance-Critical Applications*

Pritha Choudhury  
*India R&D Center*

*Alpha Assembly Solutions, a MacDermid  
Performance Solutions Business  
Bangalore, India*

[pritha.choudhury@alphaassembly.com](mailto:pritha.choudhury@alphaassembly.com)

Suresh Telu  
*India R&D Center*

*Alpha Assembly Solutions, a MacDermid  
Performance Solutions Business  
Bangalore, India*

[sureh.tel@alphaassembly.com](mailto:sureh.tel@alphaassembly.com)

Anil Kumar  
*India R&D Center*

*Alpha Assembly Solutions, a MacDermid  
Performance Solutions Business  
Bangalore, India*

[anil.kumar@alphaassembly.com](mailto:anil.kumar@alphaassembly.com)

Morgana Ribas  
*India R&D Center*

*Alpha Assembly Solutions, a MacDermid  
Performance Solutions Business  
Bangalore, India*

[morgana.ribas@alphaassembly.com](mailto:morgana.ribas@alphaassembly.com)

Siuli Sarkar  
*India R&D Center*

*Alpha Assembly Solutions, a MacDermid  
Performance Solutions Business  
Bangalore, India*

[siuli.sarkar@alphaassembly.com](mailto:siuli.sarkar@alphaassembly.com)

## Abstract

Increased complexity of interconnection metallurgies, and additional demand for higher functionality and performance have been driving novel designs and electronics miniaturization. Consequently, higher I/O's density, finer pitches and smaller package sizes are also changing the requirements of Pb-free solder alloys. Hence, there is a need for solder alloys with thermal and mechanical reliability better than SAC305, but with lower, similar or higher melting temperatures, depending on the application. In this paper, we characterize various high reliability solder alloys using uniaxial tensile tests (at different temperatures and strain rates) and creep tests. Alloying additions are used for controlling the growth of intermetallic compounds and microstructure strengthening. Major additions impact the melting behavior and the bulk mechanical properties, whereas minor alloying additions influence the diffusion kinetics and have significant impact on their thermal reliability. The uniform distribution of intermetallics minimizes dislocation motion and deformation, resulting in alloy strengthening.

Compared to SAC305, the high and ultra-high reliability alloys presented here show superior mechanical properties. The effect of temperature and strain rate on the mechanical behavior of these alloys are investigated by uniaxial tensile tests at room temperature and 150°C, and strain rates from  $10^{-4}$  to 5/s. Deformation during thermal cycling up to 150°C is expected to be controlled by creep, due to the high homologous temperature. Thus, high temperature creep test is used for estimating thermomechanical properties and longer reliability of these alloys in actual usage. As the melting behavior of these alloys cover a wide range of melting temperatures, they can be used in various applications, such as assembly of heat sensitive packages, automotive under-the-hood, semiconductors, LEDs and power electronics.

*Keywords*—Microstructure, strengthening, creep, tensile, thermomechanical reliability.

## I. INTRODUCTION

Restrictions in using Pb in soldering materials due to its toxic nature have propelled the use of Pb-free soldering materials [1-4, 5, 6]. Besides, its unique combination of electrical, chemical, physical, thermal and mechanical properties, eutectic Sn-Pb solders with relatively lower melting point (183°C) had a series of advantages [4, 7]. Besides the low material cost and savings in energy, perhaps the most significant were that lower reflow temperatures enabled using cheaper substrates and components [5, 8 - 10].

Nowadays the use of lead-free soldering materials has become widespread, either due to environmental directives or pressure from the end users [1-4]. There is an increasing complexity of interconnection metallurgies, and additional demand for higher functionality and performance are driving manufacturers to miniaturize their products [11, 7]. However, due to electronics miniaturization and novel designs, the range of requirements for Pb-free alloys is also changing [12]. With higher I/O's density, finer pitches and smaller package sizes, the reliability of solder joints becomes an issue because of increasing mechanical and thermomechanical loading [10, 13].

The automotive environment is one of the toughest since it can include extreme exposure conditions, including

chemicals, wide temperature ranges, vibration, and humidity [6, 14]. In such environments, electronic systems can also be exposed to high temperature and vibration during the automobile service-life [15]. Automotive electronics can be broadly divided in in-cabin electronics, exterior lighting, peripheral vision and detection systems, and powertrain/chassis. Most of in-cabin electronics are normally used in the temperature range of -40 to +85°C, in which SAC305 is commonly used [5, 6]. However, current trends in the automotive electronics industry are pushing the temperature limits for electronic components to the limit. There is an increasing number of electronic controls and sensors in automotive vehicles that must work in high-temperature environments [16]. Indeed, power dissipation in hybrid and fuel cell electric vehicles will increase the demand for high temperature power electronics [16]. Harsh thermal conditions of an under-the-hood automobile environment require sophisticated design methods, materials and tools to give reliable and cost-effective packaging [17]. For such electronics exposed to environments at 150°C or higher temperatures, traditional Pb-free solders like SAC305 or SAC387 may not fulfil ideal thermomechanical reliability requirements. In addition to that, there may be cases in which interconnects are exposed to high junction temperatures, but reflow temperatures lower than SAC are required for their assembly.

In this paper, we characterize various high reliability solder alloys using uniaxial tensile tests (at different temperatures and strain rates) and creep tests. The results of uniaxial tensile tests can predict the maximum load that an alloy can withstand till fracture, and by testing the alloys at various temperatures and strain rates, different types of stresses can be evaluated. In actual applications, solder joints are often exposed to high temperatures as well as high strain rates such as dropping of portable electronic devices or automotive crash situations. Slow strain rate deformation can be used to simulate situations in which the assembly undergoes change in temperature while there is a mismatch of CTE at the solder joints. Creep of solder interconnects during thermal cycling occurs when the assembly undergoes cyclic stresses due to mismatch of coefficient of thermal expansion (CTE) during cyclic temperature exposure of solder joints. The damage during creep accumulates in the solder rather than in the components to which it is joined. Additionally, the mechanism of damage during thermomechanical fatigue is likely to be like the one during creep deformation. If the solder is unable to accommodate the creep damage, the joined components deform or fracture [13].

To achieve high resistance to thermal fatigue, solder alloys are required to have high temperature creep resistance, which can be attained by combining solid solution strengthening and precipitation/ dispersion hardening to improve the mechanical strength of metallic Sn [18]. Bi, In and Sb are elements with higher solid solubility in Sn. These elements can contribute, in various degrees, towards solid solution strengthening of the Sn matrix. The alloys used in

this study have a wide range of compositions, including Sb and In additions. Low and high strain rates tensile tests are performed at ambient and 150°C, for simulating various thermomechanical reliability requirements.

## II. EXPERIMENTAL PROCEDURE

A generic description of the alloys studied here is showed in Table 1. All the alloys are SAC based, having Bi additions in varying proportions (from 0.5 to 4 wt%). Alloys 2 and 5 contain between 1 and 12 wt% Sb additions, in the lower and the higher ranges, respectively. Instead of Sb, alloy 3 has a combination of micro-alloying additions, whereas alloy 4 contains In. All these alloys contain one or two minor alloying additions (X) up to 0.2 wt%. SAC305 is also evaluated for performance comparison.

Table 1: Generic description of the alloys

Alloy ID	Generic Description
SAC305	96.5Sn-3Ag-0.5Cu
2	Sn-Ag-Cu-Sb-Bi-X
3	Sn-Ag-Cu-Bi-X
4	Sn-Ag-Cu-Bi-In-X
5	Sn-Ag-Cu-Sb-Bi-X

Alloys were prepared using a liquid metallurgy route, at a superheat of 50°C. The compositional analysis was done by ICP-OES, and the melting behavior was studied using a differential scanning calorimeter (DSC) as per ASTM E794 standard. Samples were heated at a rate of 10°C/ min to determine the solidus and liquidus temperatures.

The microstructural analysis of the alloys was done using a scanning electron microscope (SEM). Additionally, the elemental composition of the samples was qualitatively identified using Energy Dispersive X-Ray Spectroscopy (EDS).

Hardness was measured using a microhardness tester at an applied load of 1 kg. CTE measurements were done using a thermal mechanical analyzer, as per the RT-500C standard. A scan rate of 2°C/ min in the temperature range of 30 to 100°C was used.

Tensile tests were carried out using a universal testing machine (Model 5566), whereas specimens were prepared as per ASTM E8 tensile test standard. Circular specimens of 16 mm gage length (L), 4.01 mm gage diameter (D), and 3 mm shoulder radius (R) (Fig. 1) were used for the tests. Measurements were performed at two temperatures, 25 and 150°C, and three different strain rates,  $10^{-4}$ ,  $10^{-3}$  and  $5 \text{ s}^{-1}$ . These strain rates correspond to crosshead speeds of 0.096, 0.96 and 480 mm/min, respectively.

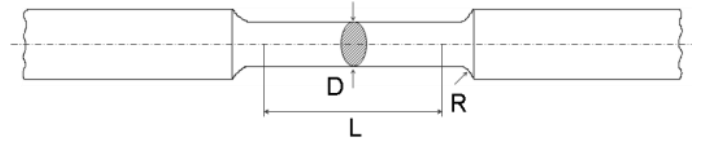


Fig. 1: Specimen geometry used for the tensile tests

For the creep test, round-threaded samples with 9 mm gage length and 6 mm diameter were machined as shown in Fig. 2. Samples were cleaned with IPA and heat treated at 125°C for 48 hours prior to testing. The testing temperature was selected so that the homologous temperature would be equal or lower than 0.85, while the testing load (200N) was selected such as to enable discrimination among the tested alloys.

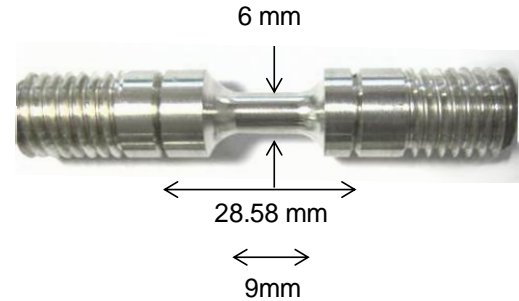


Fig. 2: Specimen for creep test

Elastic properties were measured using the ultrasonic pulse-echo technique. The elastic modulus and Poisson ratio are determined through computations based on measured sound velocities and material density. We use an ultrasonic thickness gage, and longitudinal and shear wave transducers to measure the sound velocities through the alloys. Through this technique the elastic modulus can be evaluated without the variability often observed when performing tensile tests.

## III. RESULTS AND DISCUSSION

### A. Microstructures & Physical Properties

The microstructures of the as-cast alloys are shown in Fig.3. SAC305 has eutectic  $\text{Ag}_3\text{Sn}$  interspersed with the  $\beta\text{-Sn}$  grains. Alloy 3 has much finer precipitates of  $\text{Ag}_3\text{Sn}$  than alloy 2. The long needles of  $\text{Ag}_3\text{Sn}$  in alloy 2 are more likely to develop cracks at their sharp tips than the finer counterparts in alloy 3. Distribution of the precipitates along the grain boundaries in alloy 3 would be especially helpful in strengthening the alloy against high temperature creep deformation. The dark precipitates correspond to  $\text{Cu}_6\text{Sn}_5$ . Alloy 4 has smaller eutectic colonies compared to SAC305. Additionally, alloy 5 is characterized by large cuboidal precipitates of  $\text{SnSb}$  (consisting of nearly 1:1 ratio of Sn:Sb), which would further enhance the strength of this alloy.

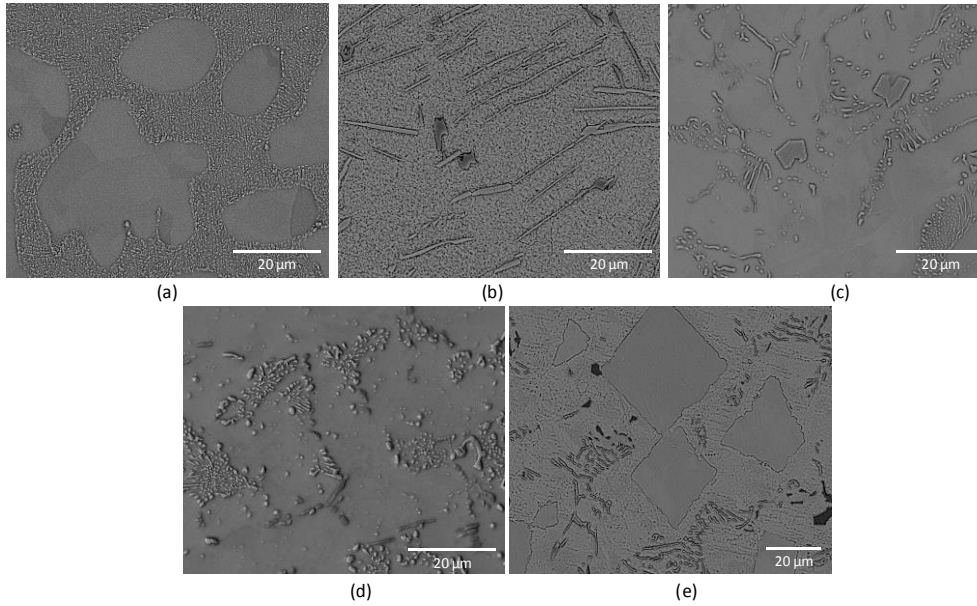


Fig. 3: Microstructures of the alloys: (a) 96.5Sn-3Ag-0.5Cu, (b) Sn-Ag-Cu-Sb-Bi-X, (c) Sn-Ag-Cu-Bi-X, (d) Sn-Ag-Vu-Bi-In-X and (e) Sn-Ag-Cu-Sb-Bi-X.

Few trends can be observed from the analysis of the physical properties of these alloys, as shown in Table 2. The melting behavior, viz. solidus and liquidus temperatures, is a decisive property for guiding high temperature reliability of solders. Lower melting temperature is desirable for enabling lower processing temperatures, consequently reducing energy consumption. However, changes in alloy composition for doing that need to be carefully done to avoid drastically reducing the corresponding solder joint thermal reliability.

Addition of Bi, as in alloys 2 and 3 reduces the solidus temperature below SAC305 level. In the case of alloy 3, the solidus temperature is reduced further by Sb removal. On the other hand, addition of higher Sb content increases the solidus and liquidus temperatures beyond SAC305, as is the case of alloy 5. As Bi addition above 5 wt.% would result in increased brittleness and poor thermomechanical reliability, In was used to further reduce the melting temperature of alloy 4.

The hardness values of alloys 2, 3, 4 and 5 are considerable higher than in SAC305. Solid solution as well as precipitation strengthening mechanisms are evident in the significant increase in hardness of these alloys. Although there are marginal differences among the moduli, alloys 2, 4 and 5 lower moduli indicates a small reduction in stiffness. This combination of apparently negative or positive properties is very important when considering alloys with multi-additives, as is the case here. Higher thermomechanical reliability will derive from a combination of strength and ductility, to better withstand creep and CTE mismatch stresses.

### B. Tensile Properties

The variation of ultimate tensile strength (UTS) and yield strength (YS) of all alloys as a function of crosshead speed (and consequently strain rate) at room temperature and 150°C is shown in Fig. 4 and 5, respectively.

Table 2: Properties of all alloys

Properties	Alloys				
	SAC305	2	3	4	5
Melting Range (°C)	217-220	215-220	209-220	192-203	221-266
Density (gm/cm <sup>3</sup> )	7.3	7.5	7.5	7.5	7.3
Hardness (HV-1)	15	31	28	29	26
CTE (μm/mK) (50-100°C)	22	25.8	23.8	25.5	22.7
CTE (μm/mK) (100-150°C)	22.3	26.2	25.5	28.6	22.9
Young's Modulus (GPa)	49.9	46.5	49.7	45.6	44.5
Shear Modulus (GPa)	18.3	16.9	18.3	16.5	16.1
Poisson's Ratio	0.36	0.38	0.36	0.38	0.38

SAC305 has considerably lower UTS and YS at both room temperature and 150°C, at the various strain rate conditions. The other alloys (2, 3, 4 and 5) have at least 50% higher tensile strength than SAC305 at room temperature (Fig.4). The standard deviation for UTS and YS at room temperature is in the range of 1 to 3 MPa. The UTS at the lowest strain rate of alloys 4 and 5 is higher than of alloys 2 and 3, whereas only alloy 5 is slightly higher at mid-strain rate, and they are mostly comparable (alloy 3 slightly lower) at the highest strain rate. The YS of alloy 5 at the lowest strain rate is higher than of alloys 2 and 3, whereas 2, 3, 4 and 5 are comparable at the mid-strain rate. However, there is a clear trend in YS at the highest strain rate, in which  $2 < 3 < 4 < 5$ . The effect of solid solution and precipitation strengthening mechanisms on the yield strength is evident. Alloys 2, 3, 4 and 5 progressively use alloying additions such as Sb, Bi and Ag for improving the mechanical reliability of the resulting solders.

High temperature tensile tests provide some insight into the thermomechanical properties of solder alloys. At

150°C, there are minor differences among tensile strength values of alloys 2, 3 and 4 at lower and mid-strain rates (Fig.5). At this temperature, the minimum standard deviation in UTS and YS is 1 MPa, while the maximum is 4 MPa. UTS of alloy 5 is clearly higher at these strain rates, whereas both alloys 4 and 5 have considerable higher YS at the highest strain rate. These results follow an expected trend, as tensile strength generally sharply decreases at this high temperature.

The yield strength shows a trend like the UTS, in which there is little difference between 2, 3 and 4, which are marginally higher than SAC305 at lower strain rates. Only at the highest strain rate these alloys could be better differentiated; alloys 2, 3 and 4 showing much higher YS than SAC305, and alloy 5 presenting more than 200% higher YS than SAC305. Indeed, alloy 5 tensile test results indicate its better suitability for under-the-hood applications, as it combines the ability to retain strength at higher operational temperatures with high strain rate conditions.

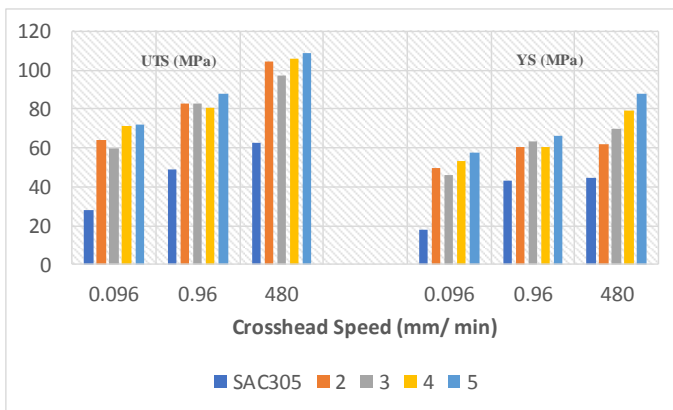


Fig. 4: Ultimate tensile strength (UTS) and yield strength (YS) as a function of crosshead speed, at room temperature.

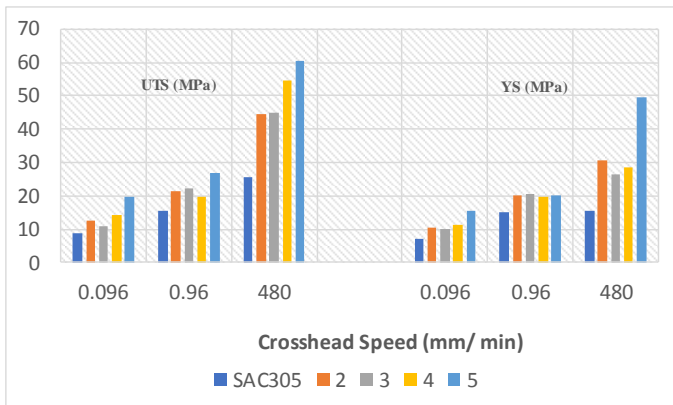


Fig. 5: Ultimate tensile strength (UTS) and yield strength (YS) as a function of crosshead speed, at 150°C.

The uniform and total elongations for all alloys under different conditions of testing are shown in Fig. 6 and 7, respectively. Uniform elongation is the elongation measured at the maximum stress and therefore is free from localized deformation that occurs during necking [19]. It is primarily

the elastic deformation along with some contribution from plastic deformation. On the other hand, total elongation is dominated by the plastic deformation added to the initial elastic deformation.

In this work, both uniform and total elongations are found to be sensitive to strain rate and temperature. Uniform and total elongation increase with increasing strain rate in SAC305 at both testing temperatures. SAC305 has a uniform distribution of the eutectic Ag<sub>3</sub>Sn in the soft and ductile β-Sn grains. That is why, the increased number of dislocations generated at higher strain rate, and their least obstructed movement, results in higher SAC305 deformation.

In the other alloys, uniform elongation increases with increasing strain rate more significantly at room temperature (Fig. 6). At higher temperature, the alloy softening results in increased ductility. At both temperatures, total elongation in these alloys decreases with increasing strain rate (Fig. 7). This implies that the large number of dislocations generated during necking are greatly hindered by the hard-intermetallic particles in their movement.

At lower strain rate, the uniform and total elongations of the other alloys remain nearly the same at both temperatures. Therefore, alloys 2, 3, 4 and 5 have similar ductility as well as similar effect of necking.

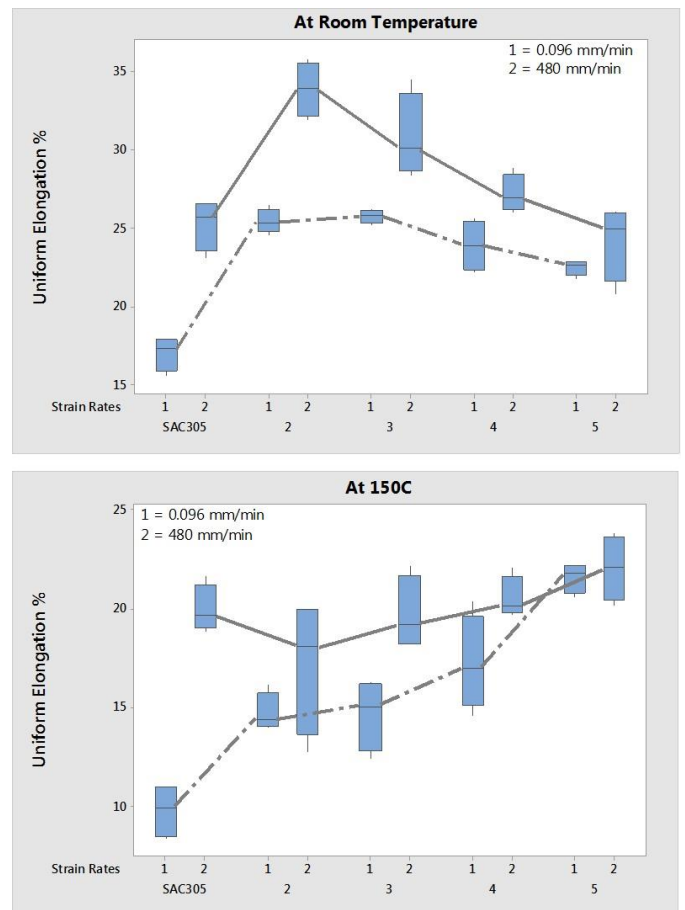


Fig. 6: Uniform elongation of the alloys as function of strain rates at room temperature (top) and 150°C (bottom).

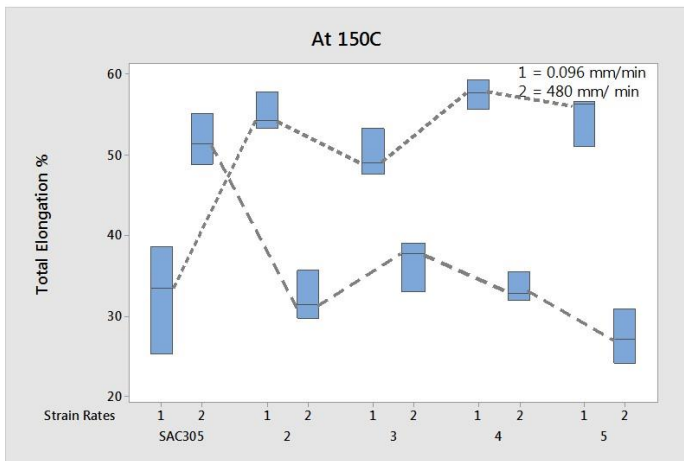
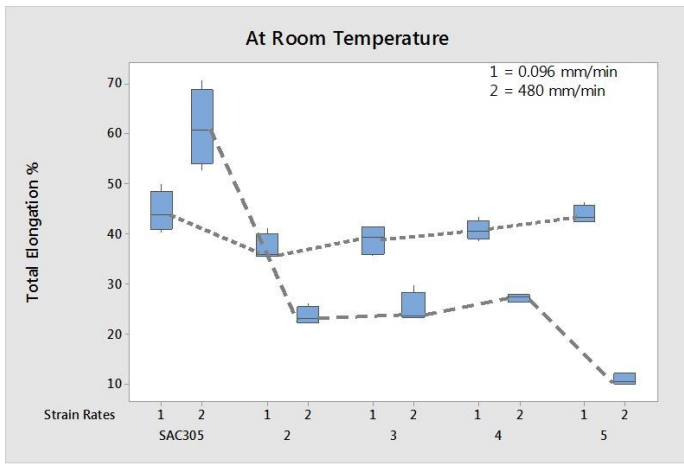


Fig. 7: Total elongation of all the alloys as a function of strain rates at room temperature (top) and 150°C (bottom).

### C. Creep

Creep strength of the alloys is expressed as creep rupture time, as shown in Fig. 8. During the high temperature creep test, the specimens are subjected to stresses lower than their respective yield stresses, but they fail due to accumulated degradation due to various mechanisms. At 150°C, the homologous temperature of SAC305, and alloys 2 and 3 is 0.86, whereas it is 0.89 for alloy 4 and 0.78 for alloy 5, so the deformation is time-dependent and controlled by creep [20].

In this case, the creep test brings additional clarity to these alloys high temperature mechanical properties. Creep rupture time results of alloys 2, 3 and 4 are within their standard deviation, but twice the creep strength of SAC305. Each of these alloys having a different combination of solid solution (Sb, Bi and/or In additions) and precipitation strengthening (Ag, Cu and/or other minor alloying additions). For example, the microstructure can be modified to form finer Ag<sub>3</sub>Sn particles and precipitates distributed along the grain boundaries that can prevent dislocation movement during creep.

Creep deformation resistance of alloy 5 is about four times larger than SAC305, and 40% larger than alloys 2, 3 and 4. One of the differentials is that alloy 5 has a larger amount of

Sb content, which contributes to solid solution as well as precipitation hardening by the formation of SbSn particles. This, in combination with having the benefits from Ag, Cu, Bi and other alloying additions, give alloy 5 its superior high temperature creep properties and are expected to translate into higher thermomechanical properties and longer reliability in actual applications. However, it is important to note that as this is a thermally activated process that was accelerated by applying stresses just below the yield strength of the material. Thus, normal operational conditions may differ and result in slower degradation or degradation over a very long period of time.

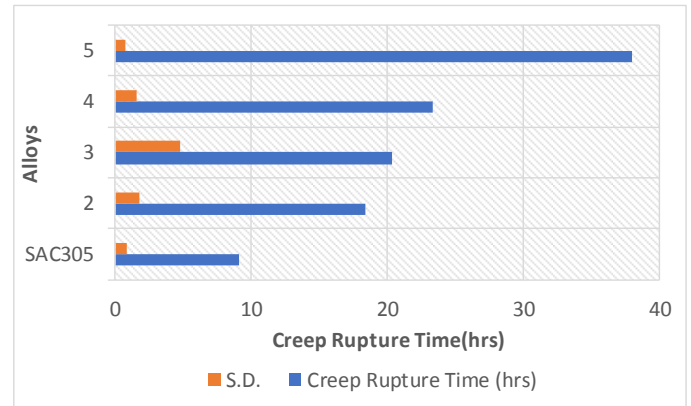


Fig. 8: High temperature creep resistance of all alloys

## IV. CONCLUSIONS

High reliability Pb-free solder alloys are strongly desirable for various applications in the electronics industry. We show here that high temperature tensile and creep tests under various conditions can be used for judging the long-term reliability of such alloys. Key conclusions are:

- Microstructure strengthening mechanisms include solid solution and precipitation strengthening, induced by a suitable choice of micro additives to achieve the desirable properties.
- Major and minor alloying additions contribute to intermetallics formation and strength retention at high temperatures.
- Alloys 2, 3 and 4 have twice the creep strength of SAC305 and can be used for various high reliability applications, such as automotive, high performance LEDs and semiconductor packaging.
- Alloy 4 can also be used for lowering reflow temperatures below 215°C, such as heat sensitive packages, second level LED assembly and hierarchical soldering.
- Alloy 5 is mostly recommended for ultra-high reliability applications, including under-the-hood, or any application requiring high temperature strength under high strain rate conditions.

Future work will include performing fatigue testing of these alloys and its validation through thermal cycling testing.

#### Acknowledgments

We thank the Metals Technology Group, Ravi Bhatkal, Ranjit Pandher, Bawa Singh and Paul Salerno for their support to this work.

#### REFERENCES

- [1] N. S. Liu and K. L. Lin, "Microstructure and mechanical properties of low Ga content Sn-8.55Zn-0.5Ag-0.1Al-xGa solders". *Scripta Materialia*, vol. 52, pp. 369-374, 2005.
- [2] N. S. Liu and K. L. Lin, "The effect of Ga content on the wetting reaction and interfacial morphology formed between Sn-8.55Zn-0.5Ag-0.1Al-xGa solders and Cu". *Scripta Materialia*, vol. 54, pp. 219-224, 2006.
- [3] J. Shen et al., "Effects of minor Cu and Zn additions on the thermal, microstructure and tensile properties of Sn-Bi-based solder alloys". *J. Alloys and Compounds*, vol. 614, pp. 63-70, 2014.
- [4] M. Abtey and Selvaduray G., "Lead-free Solders in Microelectronics", *Materials Science Eng. R*, vol. 27, pp. 95-141, 2000.
- [5] W. S. Hong, C. Oh, M. S. Kim, Y. W. Lee, H. J. Kim, S. J. Hong and J. T. Moon, "Al and Si Alloying Effect on Solder Joint Reliability in Sn-0.5Cu for Automotive Electronics". *J. Electronic Materials*, published online Aug 2016.
- [6] A. Sharma, Y. J. Jang, J. B. Kim, J. P. Jung, "Thermal cycling, shear and insulating characteristics of epoxy embedded Sn-3.0Ag-0.5Cu (SAC 305) solder paste for automotive applications". *J. Alloys and Compounds*, vol. 704, pp. 795 - 803, 15 May 2017.
- [7] R. Lim, "Investigation into Lead-free Solder in Australian Defense Force Applications". Australian Govt. Dept. Of Defense, Defense Science and Technology Organization, Air Vehicles Division, DSTO – TN – 0970.
- [8] J. W. Ronnie Teo and Y. F. Sun, "Spalling behavior of interfacial intermetallic compounds in Pb-free solder joints subjected to temperature cycling loading". *Acta Materialia*, vol. 56, pp. 242-249, 2008.
- [9] T. Laurila, V. Vuorinen, M. Paulasto-Krockel, "Impurity and alloying effects on interfacial reaction layers in Pb-free soldering". *Materials Science and Eng. R*, vol. 68, pp. 1-38, 2010.
- [10] J. G. Lee et al., "Residual-mechanical behavior of thermodynamically fatigued Sn-Ag based solder joints". *J. Electronic Materials*, vol. 31, pp. 946-952, 2002.
- [11] L. C. Tsao et al., "Effects of nano – Al<sub>2</sub>O<sub>3</sub> additions on microstructure development and hardness of Sn3.5Ag0.5Cu solder". *Materials and Design*, vol. 31, pp. 4831-4835, 2010.
- [12] P. Zimprich et al., "Mechanical size effects in miniaturized lead-free solder joints". *J. Electronic Materials*, vol. 37, pp. 102-109, 2008.
- [13] E. Lechovic, E. Hodulova, B. Szewczykova, I. Kovarikova, K. Ulrich, "Solder Joint Reliability". Institute of Production Technologies, Faculty of Materials Science and Technology, Slovak Institute of Technology, pp. 1-8.
- [14] G. Whitten, "Lead-free solder implementation for automotive electronics". Proceedings of the 50<sup>th</sup> Electronics Components and Technology Conference, 21-24 May 2000.
- [15] Pradeep Lall, Vikas Yadav, Di Zhang and Jeff Suhling, "Effect of alloy composition and aging on the survivability of leadfree solders in high temperature vibration in automotive environments". Proceedings of the ASME 2017 InterPack, pp. 1-15, 29 Aug – 01 September 2017.
- [16] R. W. Johnson and P. Jacobsen, "The changing automotive environment: high temperature electronics". *IEEE Transactions on Electronics Packaging Manufacturing*, vol. 27 (3), pp.164-176, 2004.
- [17] Walter L. Winterbottom, "Converting to lead-free solders: An automotive industry perspective". *JOM*, vol. 45 (7), pp. 20-24, 1993.
- [18] P. Choudhury et al., "New lead-free alloy for high reliability, high operating temperature conditions". Proceedings of the ICSR (Soldering and Reliability) Conference, September 2014.
- [19] Y. Cao, J. Ahlstrom and B. Karlsson, "The influence of temperatures and strain rates on the mechanical behavior of dual phase steel in different conditions", *J. of Materials Research and Technology*, vol. 4 (1), pp. 68-74, 2015.
- [20] S. Suresh, "Fatigue of Materials". Cambridge University Press: New Delhi, South Asian edition (2016), 679p.